

Supporting Information

Inter-Site Coupling and Nonlinear Density–Activity Relationship in M–N–C Single-Atom Catalysts

Xinqi Chen, Ran Shi, Haiyang Cheng, Tianci Huang, Tong Zhou, Qingju Liu, Tianwei He*

Yunnan Key Laboratory for Micro/Nano Materials & Technology, National Center for International Research on Photoelectric and Energy Materials, School of Materials and Energy, Yunnan University, Kunming 650091, China.

E-mail: he.tianwei@ynu.edu.cn

1. Calculation Methods Supplement:

1.1 Calculation of Single Metal Atom Energy E_M :

$$E_M = E_{M(bulk)}/N \# \quad (1)$$

$E_{M(bulk)}$ represents the energy of a single metal atom in the metal solid, N represents the number of atoms in the metal solid.

1.2 Calculation of Gibbs Free Energy

1.2.1 Hydrogen Evolution Reaction (HER)

To evaluate the performance of the HER, the Gibbs free energy of H adsorption (ΔG_{*H}) is calculated under standard conditions ($U = 0$ V, $pH = 0$).¹

$$\Delta G_{*H} = \Delta E_{*H} + \Delta E_{ZPE} + T\Delta S + \Delta G_U + \Delta G_{pH} \# \# \quad (2)$$

$$\Delta G_U = -eU \# \quad (3)$$

$$\Delta G_{pH} = -kT \ln_{10} * pH \# \quad (4)$$

ΔE_{*H} corresponds to the overall energy difference associated with the stable adsorption of a hydrogen atom H. ΔE_{ZPE} denotes the change in zero-point energy (ZPE) of hydrogen between its gaseous and adsorbed states. T is set to 298.15 K, and ΔS represents the change in entropy. U indicates the electrode potential relative to the standard hydrogen electrode, while e is the number of electrons transferred in each reaction step. ΔG_U refers to the voltage-dependent contribution to the Gibbs free energy, and ΔG_{pH} is the correction term that accounts for the influence of pH.

$$\Delta E_{*H} = E_{*H} - E_* - 1/2 E_{H_2} \# \quad (5)$$

E_{slab} and E_{*H} correspond to the energy of the substrate prior to and following hydrogen adsorption, respectively, E_{H_2} denotes the total energy of a hydrogen molecule in the gas phase.

$1/2 E_{H_2}$ provides an approximate representation of the energy associated with a single H atom.

$$\eta^{HER} \propto \Delta E_{*H} \# \quad (6)$$

η^{HER} represents the overpotential of the HER.

1.2.2 Oxygen Evolution Reaction (OER)

To assess the OER performance, the mechanism is described via a four-step reaction pathway.

1: A water molecule dissociates, releasing a proton pair ($H^+ + e^-$), resulting in the adsorption of

OH as the *OH intermediate; 2: The *OH releases a proton pair ($H^{++} e^-$), forming the intermediate *O. 3: a second water molecule reacts with *O, generating the *OOH intermediate. 4: *OOH releases a proton pair ($H^{++} e^-$) to produce molecular oxygen (O_2), thereby regenerating the active site of the catalyst for the next OER cycle.²

The adsorption energies of the intermediates are calculated using the following formula:

$$\Delta E_{*OH} = E_{*OH} - E_* - E_{H_2O} + \frac{1}{2}E_{H_2} \quad \# (7)$$

$$\Delta E_{*O} = E_{*O} - E_* - E_{H_2O} + E_{H_2} \quad \# (8)$$

$$\Delta E_{*OOH} = E_{*OOH} - E_* - 2E_{H_2O} + \frac{3}{2}E_{H_2} \quad \# (9)$$

The Gibbs free energies of adsorption for the three intermediates (*OH, *O, and *OOH) are

denoted by E_{*OH} , E_{*O} and ΔE_{*OOH} , respectively. The total energies of *OH, *O, and *OOH adsorbed on the catalyst are represented by ΔE_{*OH} , ΔE_{*O} and ΔE_{*OOH} . While the Gibbs free energies of the bare catalyst, H_2O , and H_2 are given by E_* , E_{H_2O} and E_{H_2} , respectively.

The change in Gibbs free energy for each step of the oxygen evolution reaction is computed according to the equations below:

$$\Delta G_1 = \Delta E_{*OH} \quad \# (10)$$

$$\Delta G_2 = \Delta E_{*O} - \Delta E_{*OH} \quad \# (11)$$

$$\Delta G_3 = \Delta E_{*OOH} - \Delta E_{*O} \quad \# (12)$$

$$\Delta G_4 = 4.92 - \Delta E_{*OOH} \quad \# (13)$$

ΔG_1 , ΔG_2 , ΔG_3 and ΔG_4 represent the Gibbs free energy changes for each step of the OER process, respectively.

To more intuitively compare the OER performance among different single-atom catalysts, the overpotential of the OER, η^{OER} is determined by identifying the potential-determining step (PDS), which corresponds to the step exhibiting the highest energy increase throughout the

reaction, and is calculated using the following expression:

$$\eta^{OER} = \max\{\Delta G_1, \Delta G_2, \Delta G_3, \Delta G_4\}/e - 1.23 \text{ (V)} \# (14)$$

1.3 Calculation of Crystal Orbital Hamilton Population (COHP):

The COHP analysis is carried out with the LOBSTER code,³ which differentiates bonding from antibonding interactions between atoms based on electron density; the integrated COHP (ICOHP) provides a quantitative measure of bond strength, where increasingly negative ICOHP values correspond to greater bonding strength.

1.4 Loading of single-atom catalysts (SACs)

Weight percentage (wt%):

$$wt\% = n_M * \frac{M_M}{n_M * M_M + n_N * M_N + n_C * M_C} \#(15)$$

Atomic percentage (at%):

$$at\% = \frac{n_M}{n_M + n_N + n_C} \#(16)$$

Where n_M , n_N , n_C represent the numbers of metal atoms, N atoms, and C atoms in the SACs, respectively; M_M , M_N , M_C denote the relative atomic masses of the metal atom, N atom, and C atom, respectively.

2.Supplementary Figures:

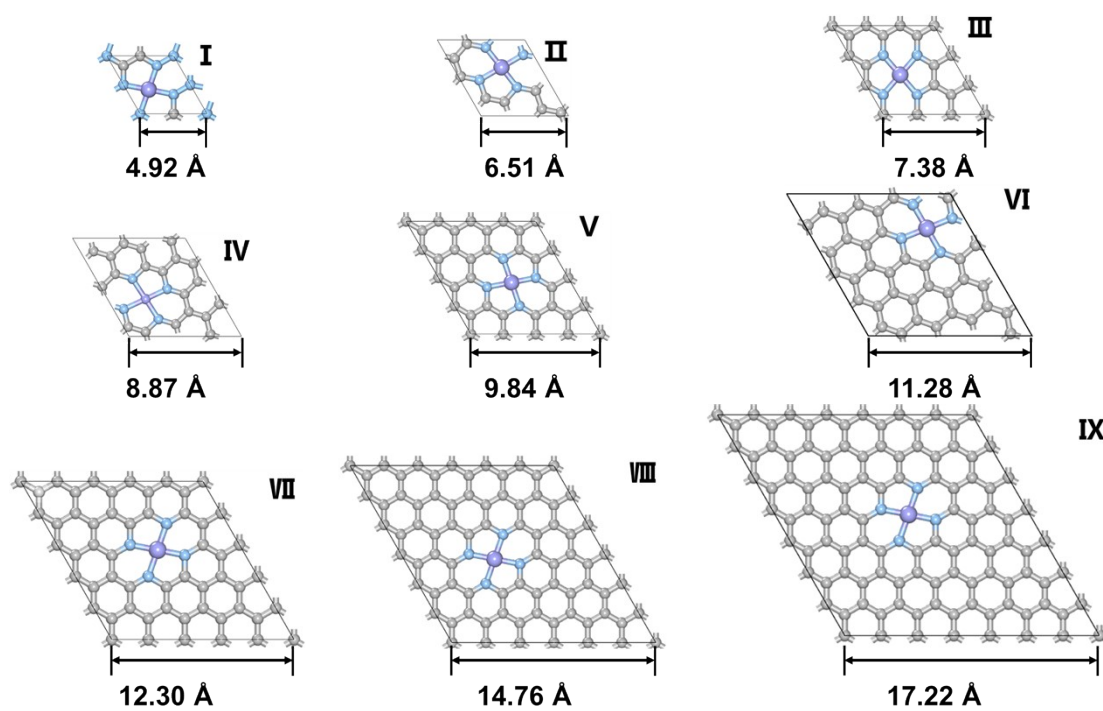


Figure S1. Unit cells of nine distinct MN₄-X structures with varying lattice sizes (X = I, II, III, IV, V, VI, VII, VIII, IX) used for DFT calculations.

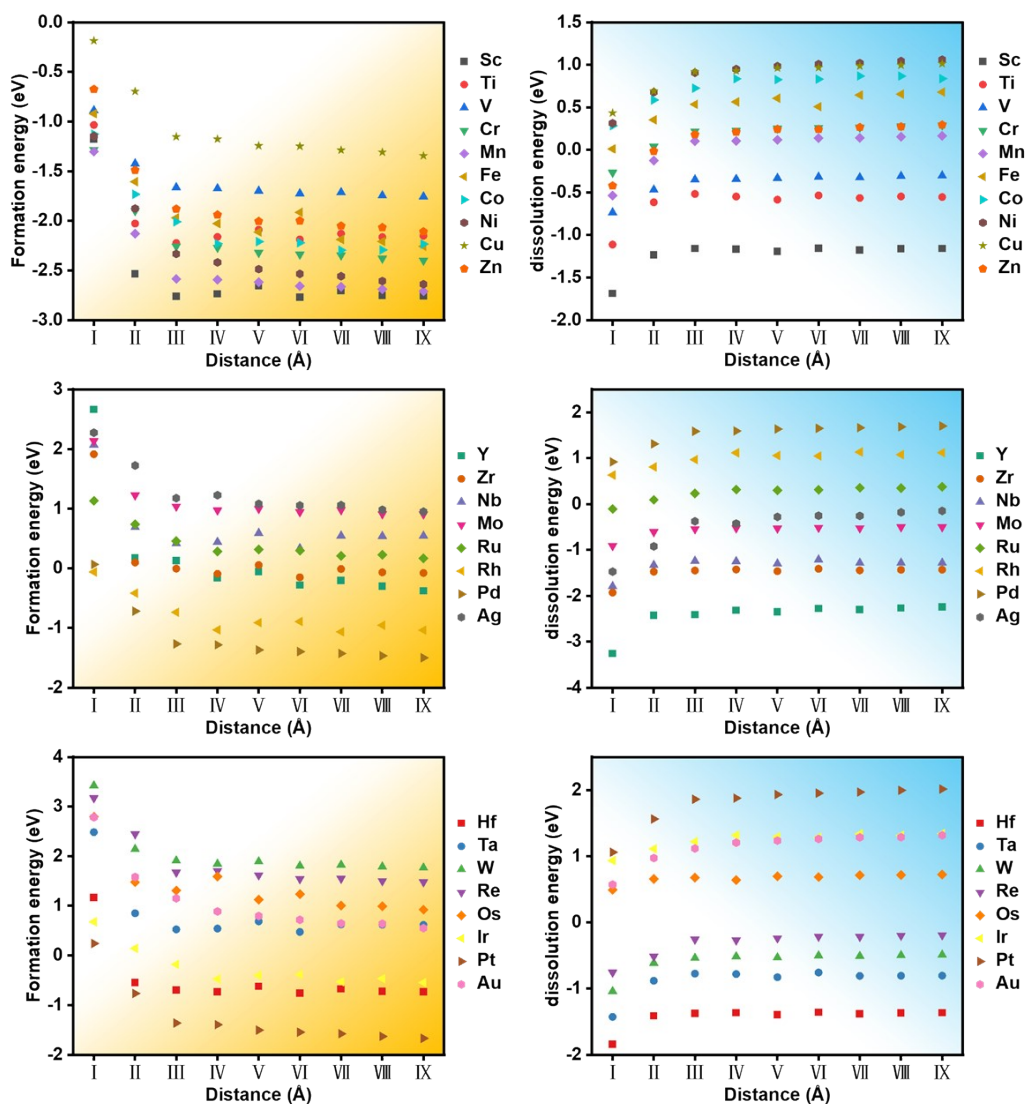


Figure S2. Formation energy and dissolution energy of 3d, 4d, and 5d metal atoms supported on different MN_4-X substrates.

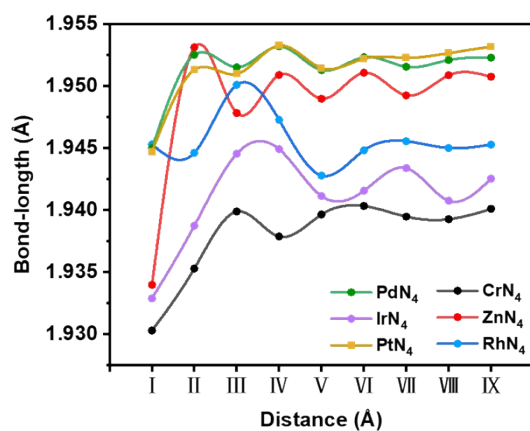


Figure S3. Variation of M–N bond length as a function of inter-metal-site distance for MN_4-X ($X = Cr, Zn, Rh, Pd, Ir, Pt$).

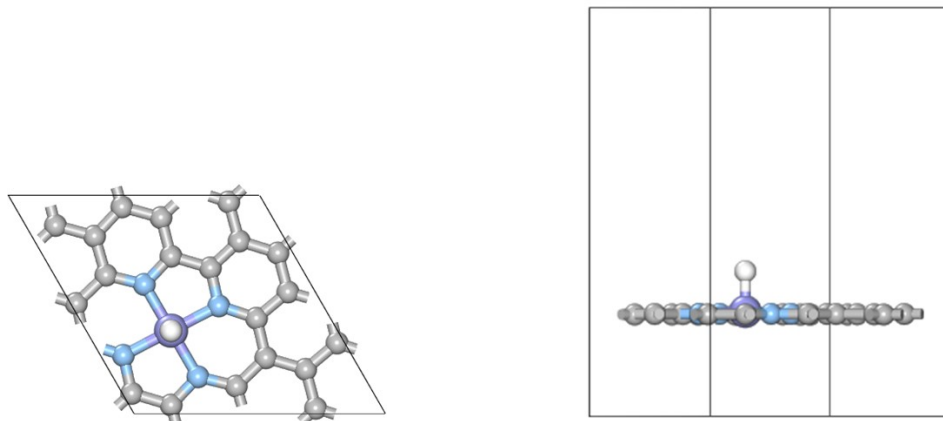


Figure S4. Stable adsorption configuration of H on MN_4 -X structures (top view and side view).

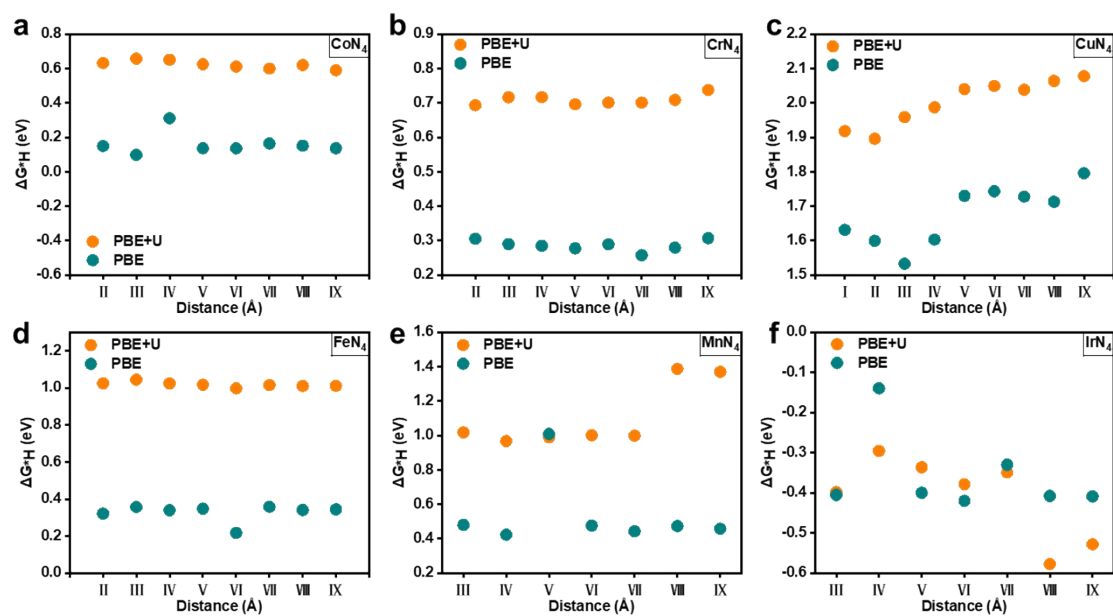


Figure S5. Comparison of HER free energy diagrams for MN_4 -X ($X = Co, Cr, Cu, Fe, Mn, Ir$) structures calculated using the PBE and PBE+U methods.

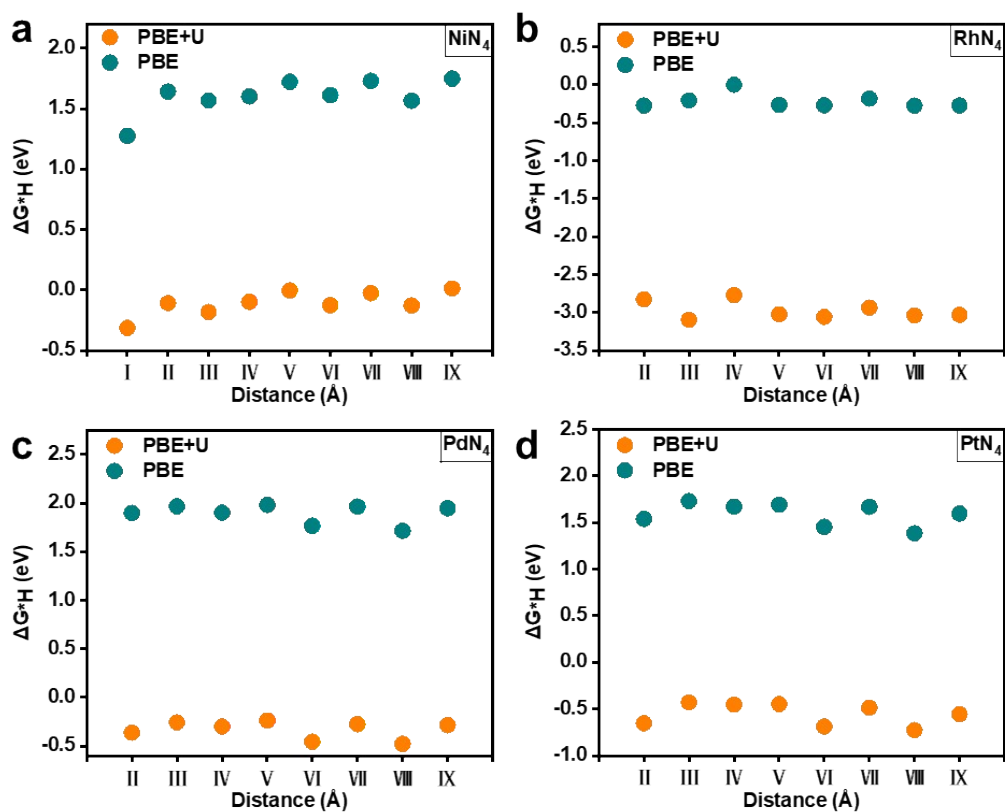


Figure S6. Comparison of HER free energy diagrams for MN_4-X ($X = Ni, Rh, Pd, Pt$) structures calculated using the PBE and PBE+U methods.

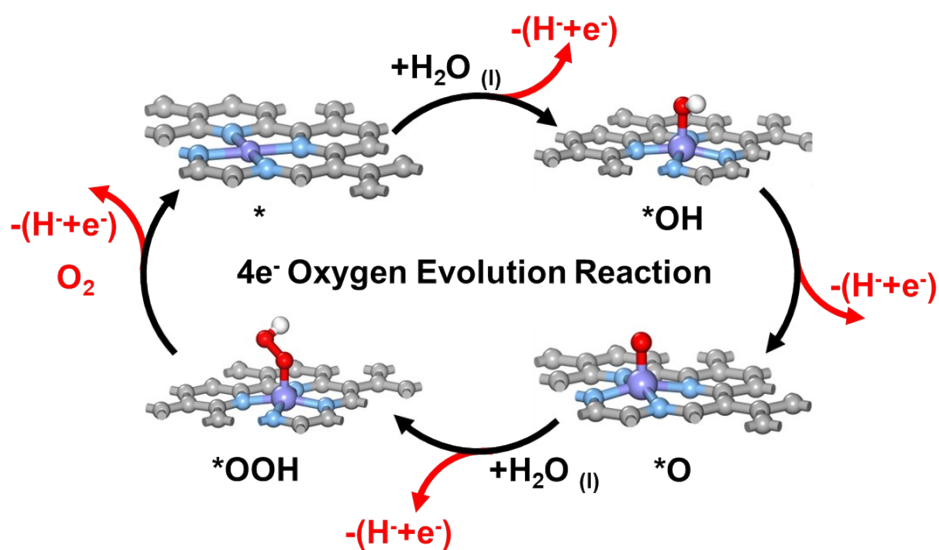


Figure S7. Reaction pathway of the $4e^-$ oxygen evolution reaction.

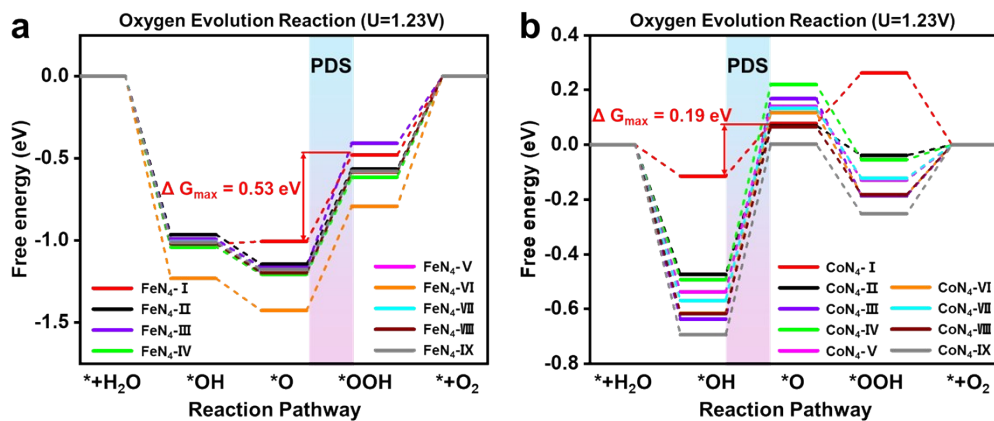


Figure S8. OER free energy diagrams of a) $\text{FeN}_4\text{-X}$ and b) $\text{CoN}_4\text{-X}$ structures calculated using the PBE method.

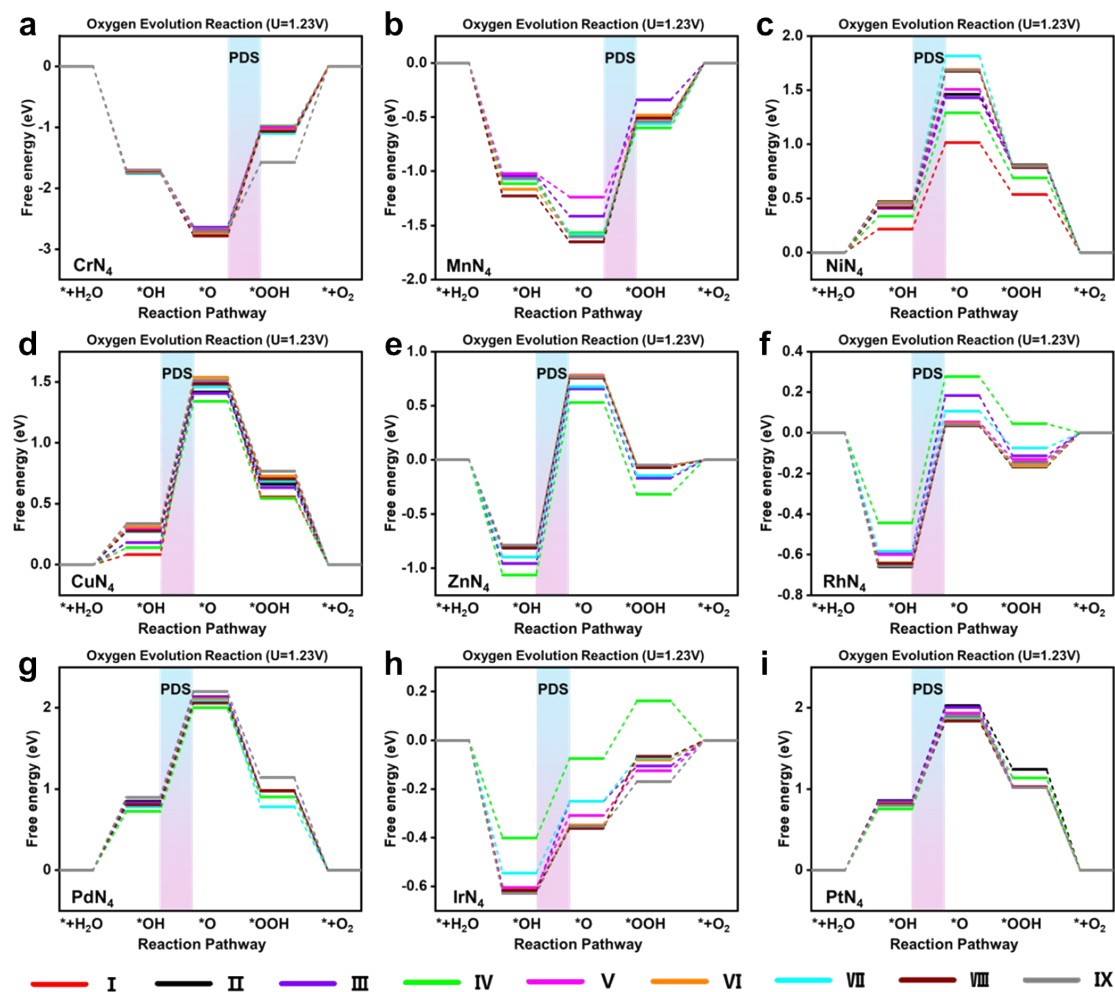


Figure S9. OER free energy diagrams of $\text{MN}_4\text{-X}$ ($\text{X} = \text{Cr}, \text{Mn}, \text{Ni}, \text{Cu}, \text{Zn}, \text{Rh}, \text{Pd}, \text{Ir}, \text{Pt}$) structures calculated using the PBE method.

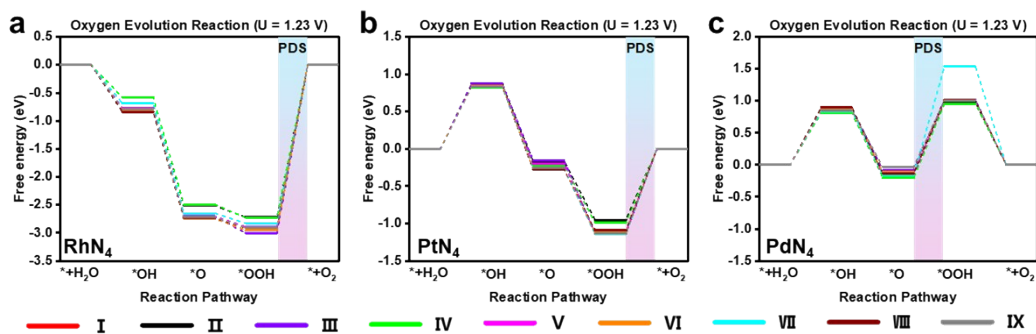


Figure S10. OER free energy diagrams of $\text{MN}_4\text{-X}$ ($\text{X} = \text{Rh}, \text{Pt}, \text{Pd}$) structures calculated using the PBE+U method.

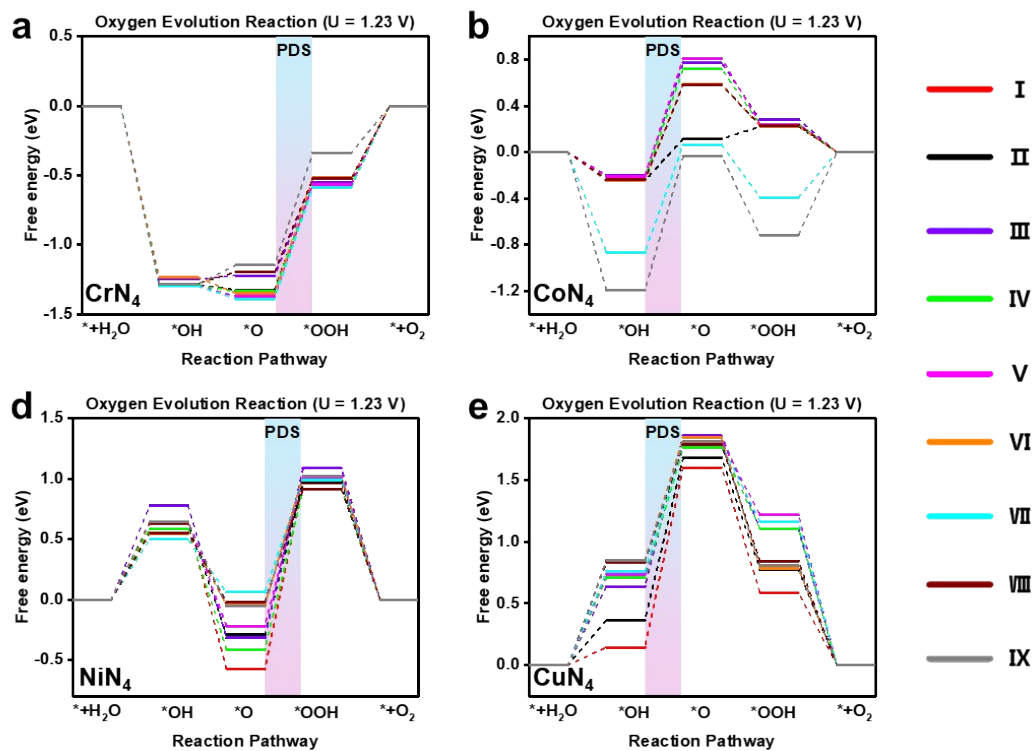


Figure S11. OER free energy diagrams of $\text{MN}_4\text{-X}$ ($\text{X} = \text{Cr}, \text{Co}, \text{Ni}, \text{Cu}$) structures calculated using the PBE+U method.

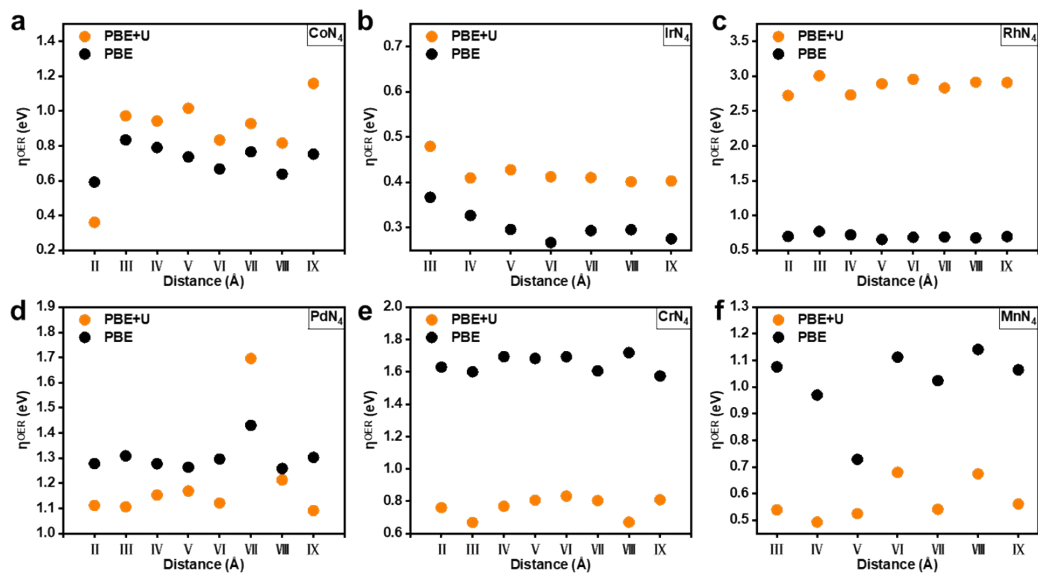


Figure S12. Comparison of OER overpotentials for $\text{MN}_4\text{-X}$ ($X = \text{Co}, \text{Ir}, \text{Rh}, \text{Pd}, \text{Cr}, \text{Mn}$) structures calculated using the PBE and PBE+U methods.

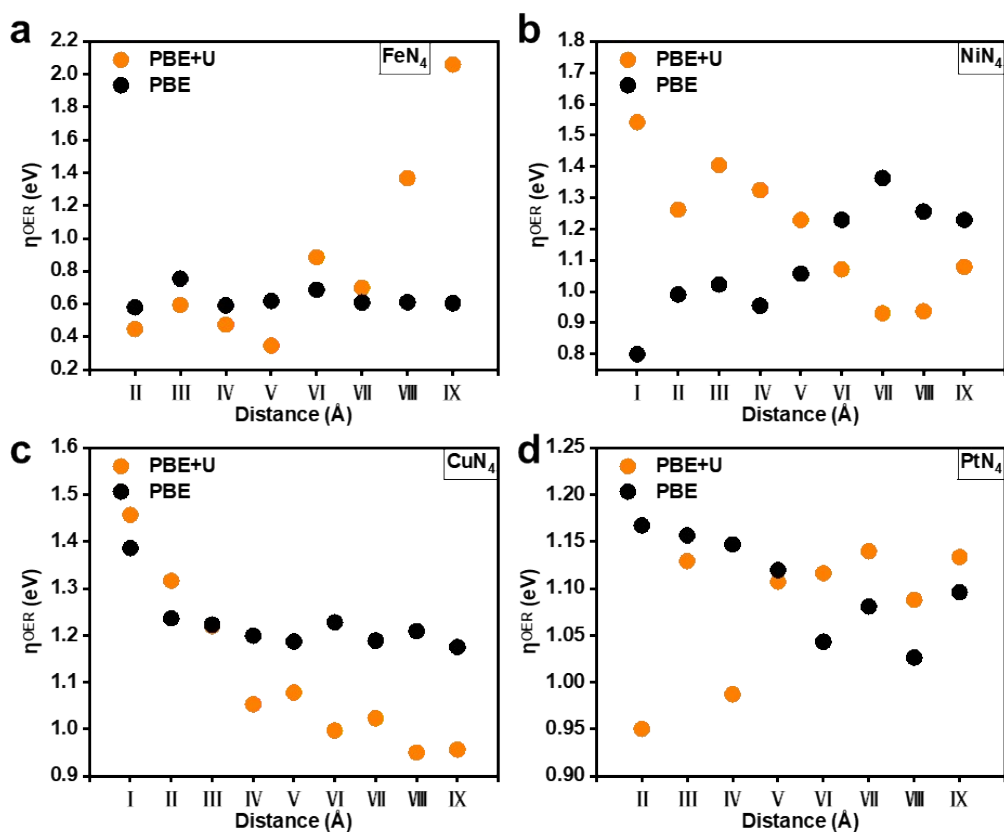


Figure S13. Comparison of OER overpotentials for $\text{MN}_4\text{-X}$ ($X = \text{Fe}, \text{Ni}, \text{Cu}, \text{Pt}$) structures calculated using the PBE and PBE+U methods.

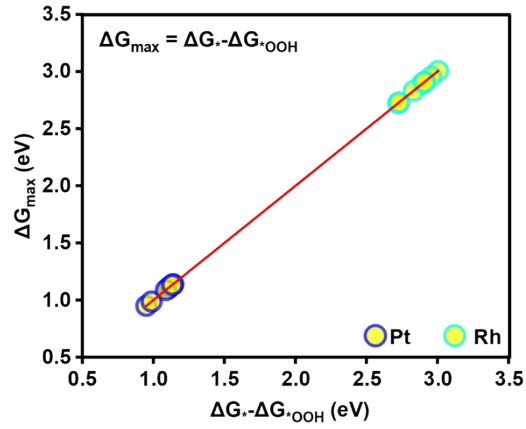


Figure S14. MN₄-X structures where OER overpotential is directly correlated with the energy of the *OOH to * step (M = Rh, Pt).

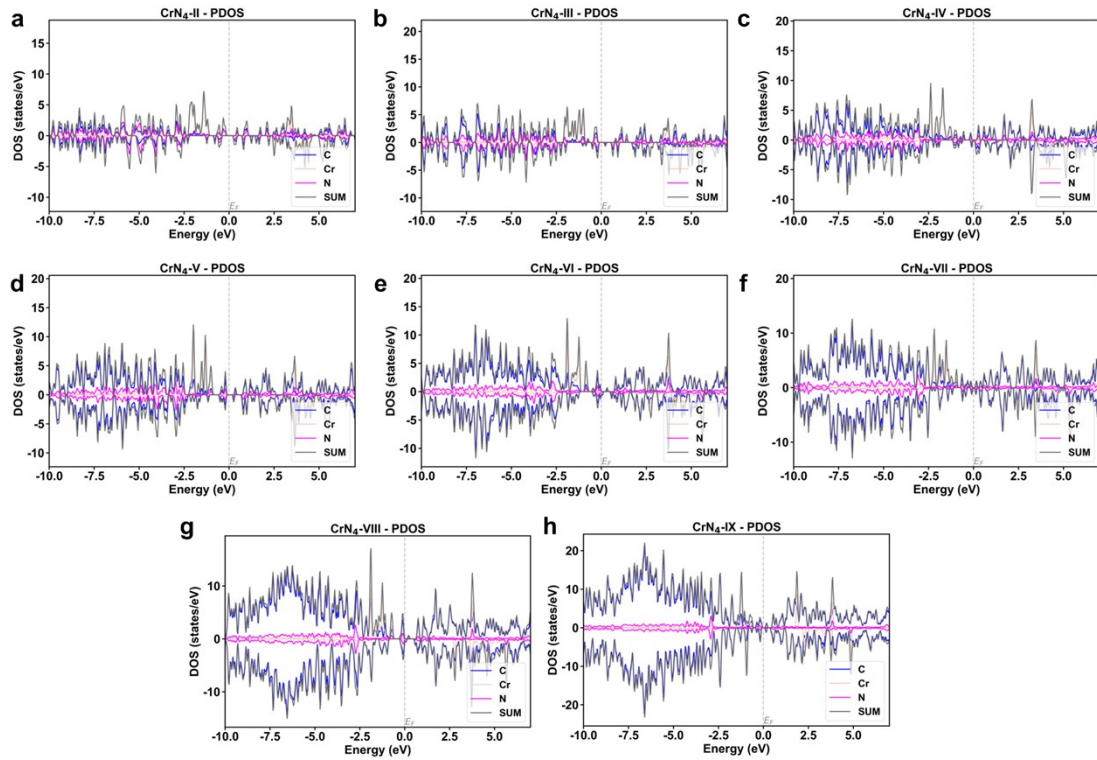


Figure S15. Density of states diagrams of CrN₄-X structures at loading densities from II to IX.

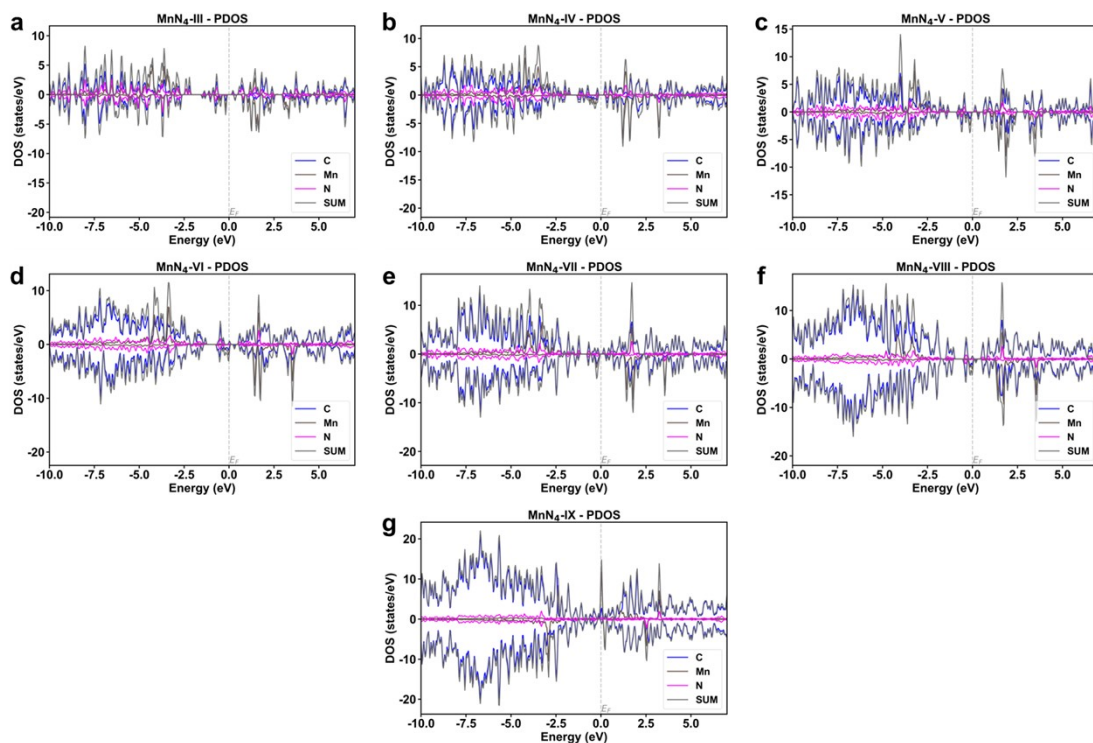


Figure S16. Density of states diagrams of $\text{MnN}_4\text{-X}$ structures at loading densities from III to IX.

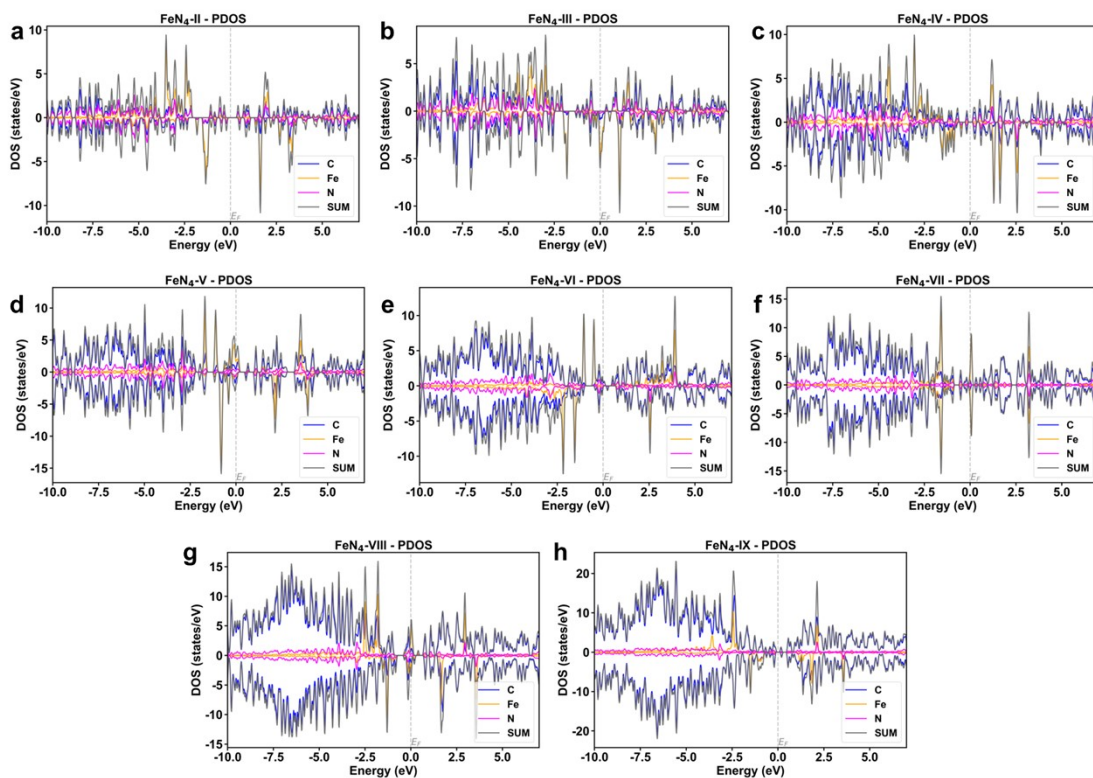


Figure S17. Density of states diagrams of $\text{FeN}_4\text{-X}$ structures at loading densities from II to IX.

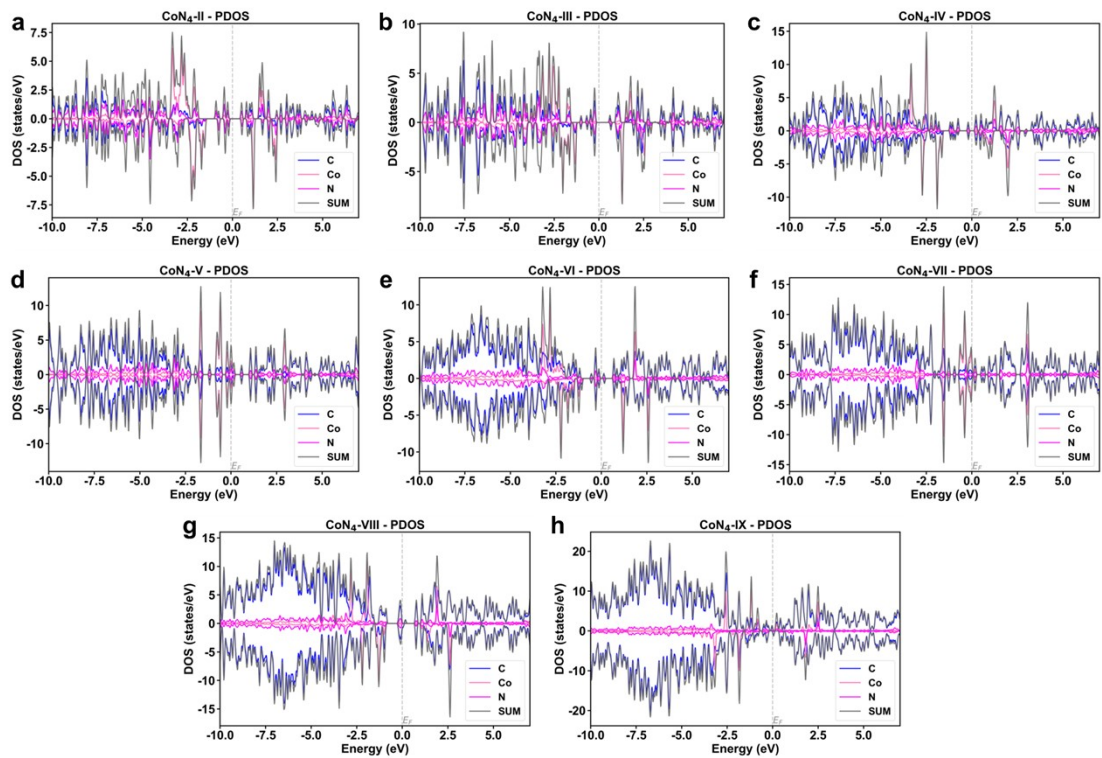


Figure S18. Density of states diagrams of $\text{CoN}_4\text{-X}$ structures at loading densities from II to IX.

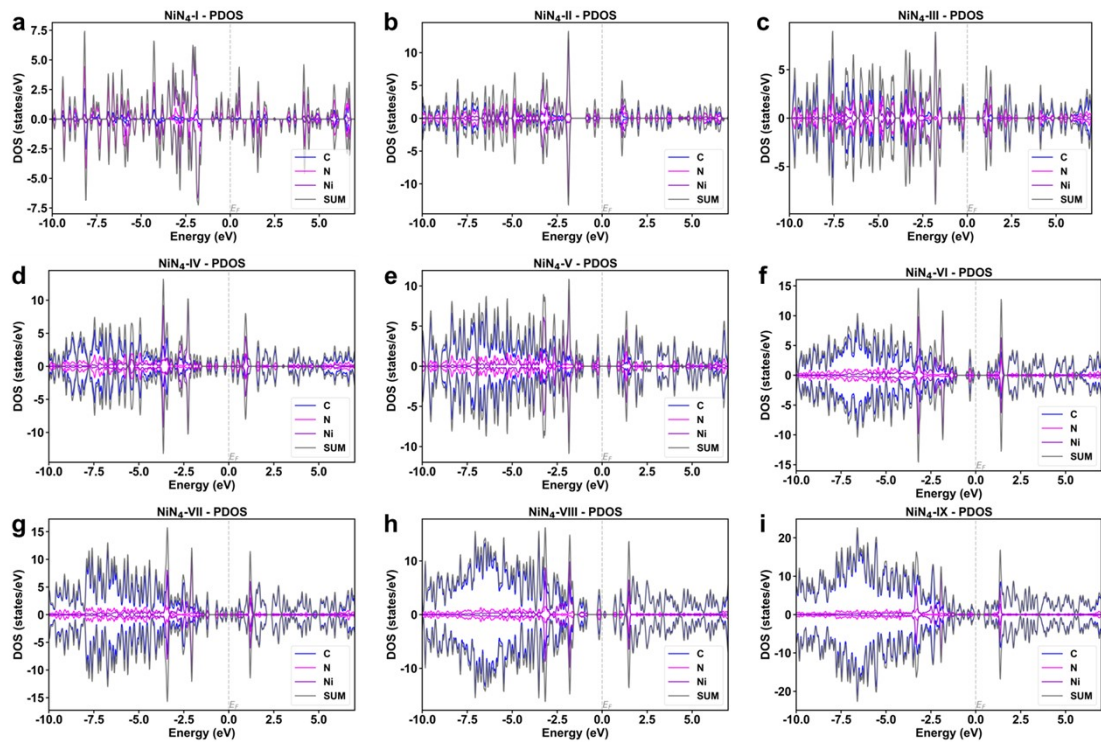


Figure S19. Density of states diagrams of $\text{NiN}_4\text{-X}$ structures at loading densities from I to IX.

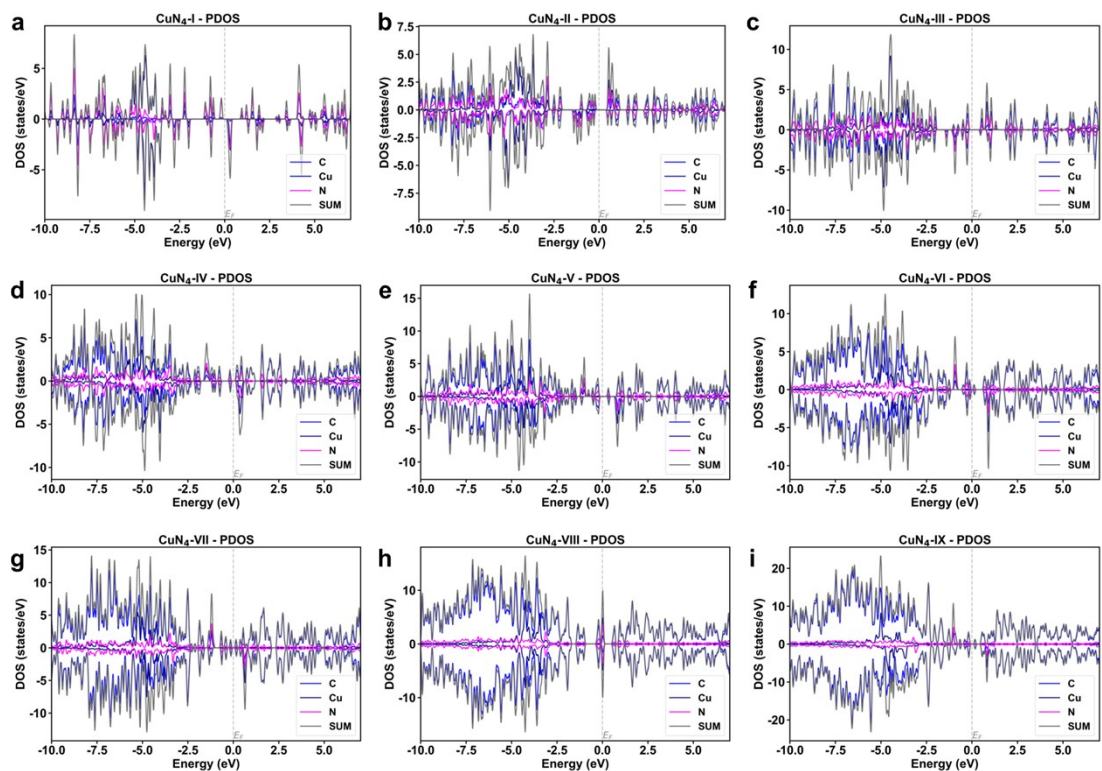


Figure S20. Density of states diagrams of $\text{CuN}_4\text{-X}$ structures at loading densities from I to IX.

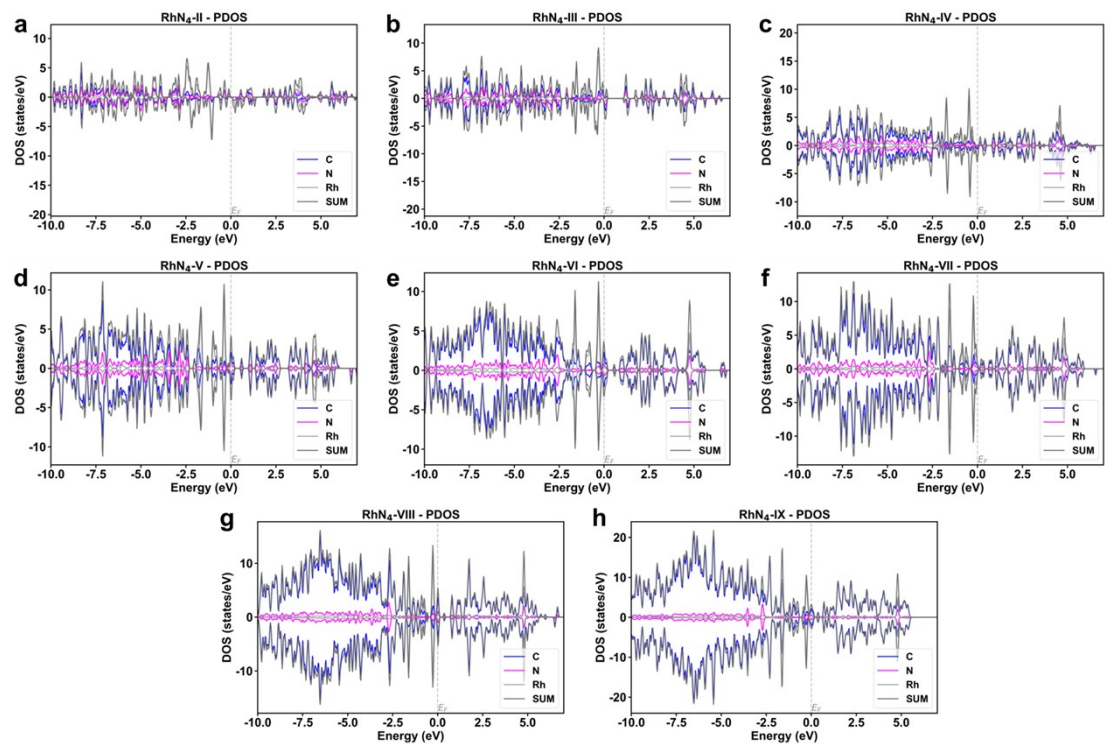


Figure S21. Density of states diagrams of $\text{RhN}_4\text{-X}$ structures at loading densities from II to IX.

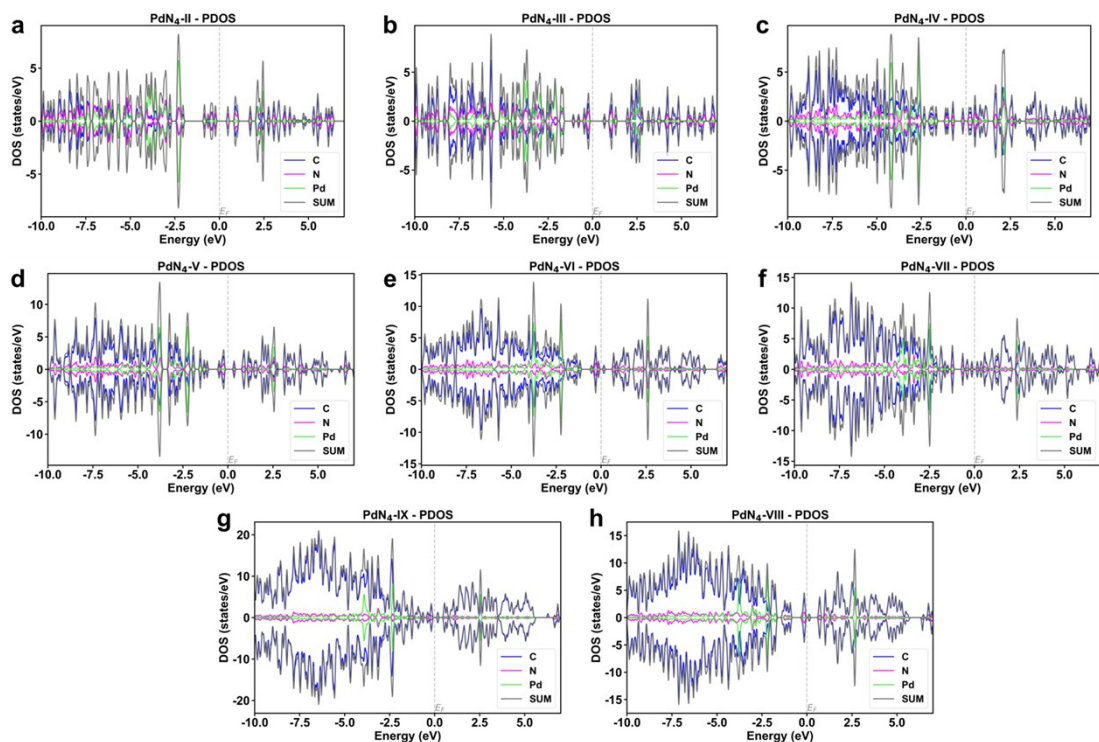


Figure S22. Density of states diagrams of PdN₄-X structures at loading densities from II to IX.

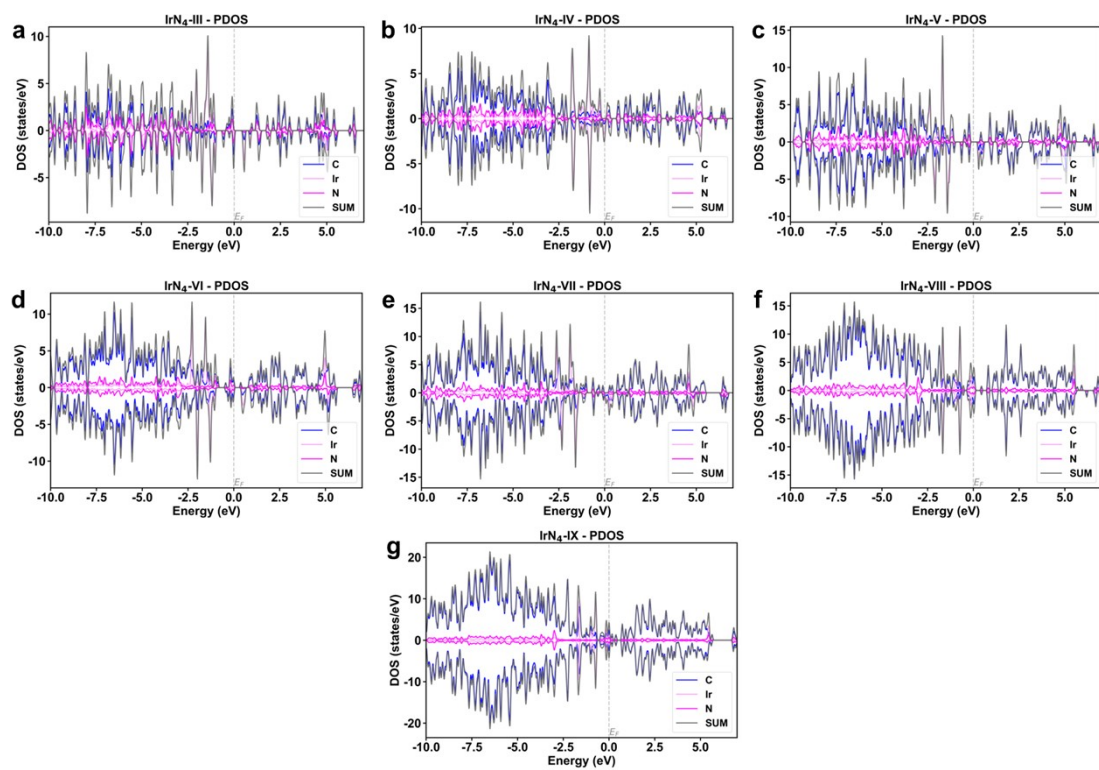


Figure S23. Density of states diagrams of IrN₄-X structures at loading densities from III to IX.

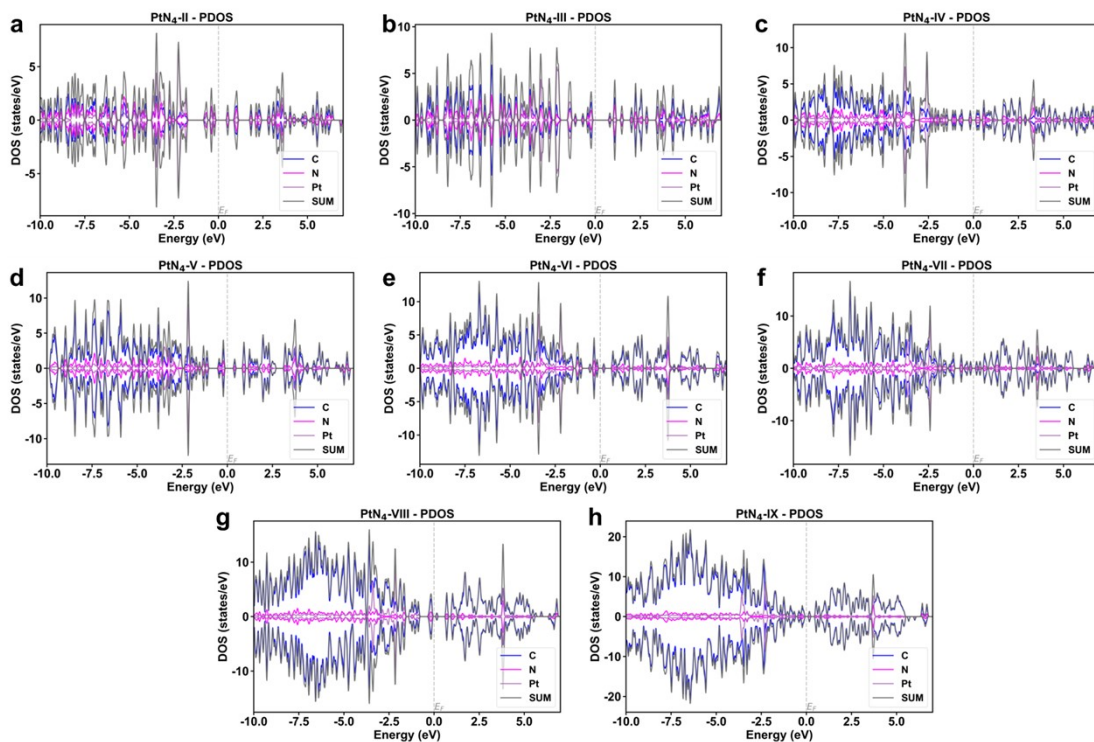


Figure S24. Density of states diagrams of $\text{PtN}_4\text{-X}$ structures at loading densities from II to IX.

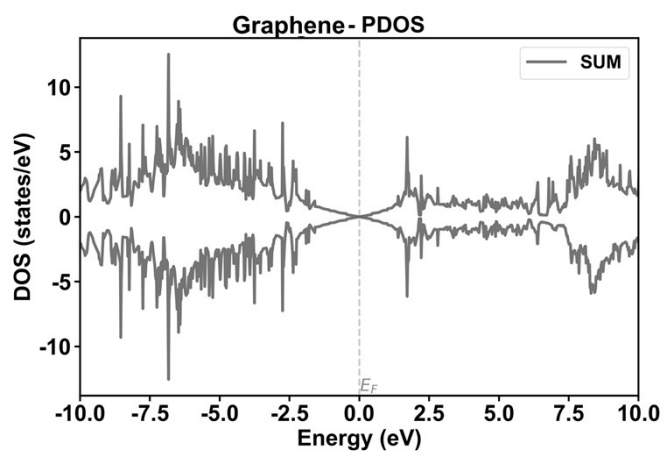


Figure S25. Density of states of the pristine graphene structure.

3 Supplementary Tables

Table S1. Weight percentage (wt%) and atomic percentage (at%) of 3d metals supported on various MN₄-X substrates.

3d-Metal	Number of N	Number of C	Number of M	Relative Atomic Mass of C	Relative Atomic Mass of N	Relative Atomic Mass of M	Weight percentage (wt%)	atomic percentage (at%)
Sc	2	4	1	12.011	14.007	44.956	0.36	0.143
Sc	8	4	1	12.011	14.007	44.956	0.23	0.077
Sc	12	4	1	12.011	14.007	44.956	0.18	0.059
Sc	20	4	1	12.011	14.007	44.956	0.13	0.040
Sc	26	4	1	12.011	14.007	44.956	0.11	0.032
Sc	36	4	1	12.011	14.007	44.956	0.08	0.024
Sc	44	4	1	12.011	14.007	44.956	0.07	0.020
Sc	66	4	1	12.011	14.007	44.956	0.05	0.014
Sc	92	4	1	12.011	14.007	44.956	0.04	0.010
Ti	2	4	1	12.011	14.007	47.876	0.37	0.143
Ti	8	4	1	12.011	14.007	47.876	0.24	0.077
Ti	12	4	1	12.011	14.007	47.876	0.19	0.059
Ti	20	4	1	12.011	14.007	47.876	0.14	0.040
Ti	26	4	1	12.011	14.007	47.876	0.12	0.032
Ti	36	4	1	12.011	14.007	47.876	0.09	0.024
Ti	44	4	1	12.011	14.007	47.876	0.08	0.020
Ti	66	4	1	12.011	14.007	47.876	0.05	0.014
Ti	92	4	1	12.011	14.007	47.876	0.04	0.010
V	2	4	1	12.011	14.007	50.942	0.39	0.143
V	8	4	1	12.011	14.007	50.942	0.25	0.077
V	12	4	1	12.011	14.007	50.942	0.20	0.059
V	20	4	1	12.011	14.007	50.942	0.15	0.040
V	26	4	1	12.011	14.007	50.942	0.12	0.032
V	36	4	1	12.011	14.007	50.942	0.09	0.024

V	44	4	1	12.011	14.007	50.942	0.08	0.020
V	66	4	1	12.011	14.007	50.942	0.06	0.014
V	92	4	1	12.011	14.007	50.942	0.04	0.010
Cr	2	4	1	12.011	14.007	51.996	0.39	0.143
Cr	8	4	1	12.011	14.007	51.996	0.25	0.077
Cr	12	4	1	12.011	14.007	51.996	0.21	0.059
Cr	20	4	1	12.011	14.007	51.996	0.15	0.040
Cr	26	4	1	12.011	14.007	51.996	0.12	0.032
Cr	36	4	1	12.011	14.007	51.996	0.10	0.024
Cr	44	4	1	12.011	14.007	51.996	0.08	0.020
Cr	66	4	1	12.011	14.007	51.996	0.06	0.014
Cr	92	4	1	12.011	14.007	51.996	0.04	0.010
Mn	2	4	1	12.011	14.007	54.938	0.41	0.143
Mn	8	4	1	12.011	14.007	54.938	0.27	0.077
Mn	12	4	1	12.011	14.007	54.938	0.22	0.059
Mn	20	4	1	12.011	14.007	54.938	0.16	0.040
Mn	26	4	1	12.011	14.007	54.938	0.13	0.032
Mn	36	4	1	12.011	14.007	54.938	0.10	0.024
Mn	44	4	1	12.011	14.007	54.938	0.09	0.020
Mn	66	4	1	12.011	14.007	54.938	0.06	0.014
Mn	92	4	1	12.011	14.007	54.938	0.05	0.010
Fe	2	4	1	12.011	14.007	55.845	0.41	0.143
Fe	8	4	1	12.011	14.007	55.845	0.27	0.077
Fe	12	4	1	12.011	14.007	55.845	0.22	0.059
Fe	20	4	1	12.011	14.007	55.845	0.16	0.040
Fe	26	4	1	12.011	14.007	55.845	0.13	0.032
Fe	36	4	1	12.011	14.007	55.845	0.10	0.024
Fe	44	4	1	12.011	14.007	55.845	0.09	0.020
Fe	66	4	1	12.011	14.007	55.845	0.06	0.014
Fe	92	4	1	12.011	14.007	55.845	0.05	0.010

Co	2	4	1	12.011	14.007	58.933	0.42	0.143
Co	8	4	1	12.011	14.007	58.933	0.28	0.077
Co	12	4	1	12.011	14.007	58.933	0.23	0.059
Co	20	4	1	12.011	14.007	58.933	0.17	0.040
Co	26	4	1	12.011	14.007	58.933	0.14	0.032
Co	36	4	1	12.011	14.007	58.933	0.11	0.024
Co	44	4	1	12.011	14.007	58.933	0.09	0.020
Co	66	4	1	12.011	14.007	58.933	0.06	0.014
Co	92	4	1	12.011	14.007	58.933	0.05	0.010
Ni	2	4	1	12.011	14.007	58.693	0.42	0.143
Ni	8	4	1	12.011	14.007	58.693	0.28	0.077
Ni	12	4	1	12.011	14.007	58.693	0.23	0.059
Ni	20	4	1	12.011	14.007	58.693	0.17	0.040
Ni	26	4	1	12.011	14.007	58.693	0.14	0.032
Ni	36	4	1	12.011	14.007	58.693	0.11	0.024
Ni	44	4	1	12.011	14.007	58.693	0.09	0.020
Ni	66	4	1	12.011	14.007	58.693	0.06	0.014
Ni	92	4	1	12.011	14.007	58.693	0.05	0.010
Cu	2	4	1	12.011	14.007	63.546	0.44	0.143
Cu	8	4	1	12.011	14.007	63.546	0.29	0.077
Cu	12	4	1	12.011	14.007	63.546	0.24	0.059
Cu	20	4	1	12.011	14.007	63.546	0.18	0.040
Cu	26	4	1	12.011	14.007	63.546	0.15	0.032
Cu	36	4	1	12.011	14.007	63.546	0.12	0.024
Cu	44	4	1	12.011	14.007	63.546	0.10	0.020
Cu	66	4	1	12.011	14.007	63.546	0.07	0.014
Cu	92	4	1	12.011	14.007	63.546	0.05	0.010
Zn	2	4	1	12.011	14.007	65.38	0.45	0.143
Zn	8	4	1	12.011	14.007	65.38	0.30	0.077
Zn	12	4	1	12.011	14.007	65.38	0.25	0.059

Zn	20	4	1	12.011	14.007	65.38	0.18	0.040
Zn	26	4	1	12.011	14.007	65.38	0.15	0.032
Zn	36	4	1	12.011	14.007	65.38	0.12	0.024
Zn	44	4	1	12.011	14.007	65.38	0.10	0.020
Zn	66	4	1	12.011	14.007	65.38	0.07	0.014
Zn	92	4	1	12.011	14.007	65.38	0.05	0.010

Table S2. Weight percentage (wt%) and atomic percentage (at%) of 4d metals supported on various MN₄-X substrates.

4d-Metal	Number of N	Number of C	Number of M	Relative Atomic Mass of C	Relative Atomic Mass of N	Relative Atomic Mass of M	Weight percentage (wt%)	atomic percentage (at%)
Y	2	4	1	12.011	14.007	88.906	0.53	0.143
Y	8	4	1	12.011	14.007	88.906	0.37	0.077
Y	12	4	1	12.011	14.007	88.906	0.31	0.059
Y	20	4	1	12.011	14.007	88.906	0.23	0.040
Y	26	4	1	12.011	14.007	88.906	0.19	0.032
Y	36	4	1	12.011	14.007	88.906	0.15	0.024
Y	44	4	1	12.011	14.007	88.906	0.13	0.020
Y	66	4	1	12.011	14.007	88.906	0.09	0.014
Y	92	4	1	12.011	14.007	88.906	0.07	0.010
Zr	2	4	1	12.011	14.007	91.224	0.53	0.143
Zr	8	4	1	12.011	14.007	91.224	0.37	0.077
Zr	12	4	1	12.011	14.007	91.224	0.31	0.059
Zr	20	4	1	12.011	14.007	91.224	0.24	0.040
Zr	26	4	1	12.011	14.007	91.224	0.20	0.032
Zr	36	4	1	12.011	14.007	91.224	0.16	0.024
Zr	44	4	1	12.011	14.007	91.224	0.13	0.020
Zr	66	4	1	12.011	14.007	91.224	0.10	0.014
Zr	92	4	1	12.011	14.007	91.224	0.07	0.010
Nb	2	4	1	12.011	14.007	92.906	0.54	0.143
Nb	8	4	1	12.011	14.007	92.906	0.38	0.077
Nb	12	4	1	12.011	14.007	92.906	0.32	0.059
Nb	20	4	1	12.011	14.007	92.906	0.24	0.040
Nb	26	4	1	12.011	14.007	92.906	0.20	0.032
Nb	36	4	1	12.011	14.007	92.906	0.16	0.024
Nb	44	4	1	12.011	14.007	92.906	0.14	0.020

Nb	66	4	1	12.011	14.007	92.906	0.10	0.014
Nb	92	4	1	12.011	14.007	92.906	0.07	0.010
Mo	2	4	1	12.011	14.007	95.95	0.55	0.143
Mo	8	4	1	12.011	14.007	95.95	0.39	0.077
Mo	12	4	1	12.011	14.007	95.95	0.32	0.059
Mo	20	4	1	12.011	14.007	95.95	0.24	0.040
Mo	26	4	1	12.011	14.007	95.95	0.21	0.032
Mo	36	4	1	12.011	14.007	95.95	0.16	0.024
Mo	44	4	1	12.011	14.007	95.95	0.14	0.020
Mo	66	4	1	12.011	14.007	95.95	0.10	0.014
Mo	92	4	1	12.011	14.007	95.95	0.08	0.010
Ru	2	4	1	12.011	14.007	101.07	0.56	0.143
Ru	8	4	1	12.011	14.007	101.07	0.40	0.077
Ru	12	4	1	12.011	14.007	101.07	0.34	0.059
Ru	20	4	1	12.011	14.007	101.07	0.25	0.040
Ru	26	4	1	12.011	14.007	101.07	0.22	0.032
Ru	36	4	1	12.011	14.007	101.07	0.17	0.024
Ru	44	4	1	12.011	14.007	101.07	0.15	0.020
Ru	66	4	1	12.011	14.007	101.07	0.11	0.014
Ru	92	4	1	12.011	14.007	101.07	0.08	0.010
Rh	2	4	1	12.011	14.007	102.91	0.56	0.143
Rh	8	4	1	12.011	14.007	102.91	0.40	0.077
Rh	12	4	1	12.011	14.007	102.91	0.34	0.059
Rh	20	4	1	12.011	14.007	102.91	0.26	0.040
Rh	26	4	1	12.011	14.007	102.91	0.22	0.032
Rh	36	4	1	12.011	14.007	102.91	0.17	0.024
Rh	44	4	1	12.011	14.007	102.91	0.15	0.020
Rh	66	4	1	12.011	14.007	102.91	0.11	0.014
Rh	92	4	1	12.011	14.007	102.91	0.08	0.010
Pd	2	4	1	12.011	14.007	106.42	0.57	0.143

Pd	8	4	1	12.011	14.007	106.42	0.41	0.077
Pd	12	4	1	12.011	14.007	106.42	0.35	0.059
Pd	20	4	1	12.011	14.007	106.42	0.26	0.040
Pd	26	4	1	12.011	14.007	106.42	0.22	0.032
Pd	36	4	1	12.011	14.007	106.42	0.18	0.024
Pd	44	4	1	12.011	14.007	106.42	0.15	0.020
Pd	66	4	1	12.011	14.007	106.42	0.11	0.014
Pd	92	4	1	12.011	14.007	106.42	0.08	0.010
Ag	2	4	1	12.011	14.007	107.87	0.57	0.143
Ag	8	4	1	12.011	14.007	107.87	0.41	0.077
Ag	12	4	1	12.011	14.007	107.87	0.35	0.059
Ag	20	4	1	12.011	14.007	107.87	0.27	0.040
Ag	26	4	1	12.011	14.007	107.87	0.23	0.032
Ag	36	4	1	12.011	14.007	107.87	0.18	0.024
Ag	44	4	1	12.011	14.007	107.87	0.16	0.020
Ag	66	4	1	12.011	14.007	107.87	0.11	0.014
Ag	92	4	1	12.011	14.007	107.87	0.09	0.010

Table S3. Weight percentage (wt%) and atomic percentage (at%) of 5d metals supported on various MN₄-X substrates.

5d-Metal	Number of N	Number of C	Number of M	Relative Atomic Mass of C	Relative Atomic Mass of N	Relative Atomic Mass of M	Weight percentage (wt%)	atomic percentage (at%)
Hf	2	4	1	12.011	14.007	178.49	0.69	0.143
Hf	8	4	1	12.011	14.007	178.49	0.54	0.077
Hf	12	4	1	12.011	14.007	178.49	0.47	0.059
Hf	20	4	1	12.011	14.007	178.49	0.38	0.040
Hf	26	4	1	12.011	14.007	178.49	0.33	0.032
Hf	36	4	1	12.011	14.007	178.49	0.27	0.024
Hf	44	4	1	12.011	14.007	178.49	0.23	0.020
Hf	66	4	1	12.011	14.007	178.49	0.17	0.014
Hf	92	4	1	12.011	14.007	178.49	0.13	0.010
Ta	2	4	1	12.011	14.007	180.95	0.69	0.143
Ta	8	4	1	12.011	14.007	180.95	0.54	0.077
Ta	12	4	1	12.011	14.007	180.95	0.47	0.059
Ta	20	4	1	12.011	14.007	180.95	0.38	0.040
Ta	26	4	1	12.011	14.007	180.95	0.33	0.032
Ta	36	4	1	12.011	14.007	180.95	0.27	0.024
Ta	44	4	1	12.011	14.007	180.95	0.24	0.020
Ta	66	4	1	12.011	14.007	180.95	0.18	0.014
Ta	92	4	1	12.011	14.007	180.95	0.13	0.010
W	2	4	1	12.011	14.007	183.84	0.70	0.143
W	8	4	1	12.011	14.007	183.84	0.55	0.077
W	12	4	1	12.011	14.007	183.84	0.48	0.059
W	20	4	1	12.011	14.007	183.84	0.38	0.040
W	26	4	1	12.011	14.007	183.84	0.33	0.032
W	36	4	1	12.011	14.007	183.84	0.27	0.024
W	44	4	1	12.011	14.007	183.84	0.24	0.020

W	66	4	1	12.011	14.007	183.84	0.18	0.014
W	92	4	1	12.011	14.007	183.84	0.14	0.010
Re	2	4	1	12.011	14.007	186.21	0.70	0.143
Re	8	4	1	12.011	14.007	186.21	0.55	0.077
Re	12	4	1	12.011	14.007	186.21	0.48	0.059
Re	20	4	1	12.011	14.007	186.21	0.39	0.040
Re	26	4	1	12.011	14.007	186.21	0.34	0.032
Re	36	4	1	12.011	14.007	186.21	0.28	0.024
Re	44	4	1	12.011	14.007	186.21	0.24	0.020
Re	66	4	1	12.011	14.007	186.21	0.18	0.014
Re	92	4	1	12.011	14.007	186.21	0.14	0.010
Os	2	4	1	12.011	14.007	190.23	0.70	0.143
Os	8	4	1	12.011	14.007	190.23	0.56	0.077
Os	12	4	1	12.011	14.007	190.23	0.49	0.059
Os	20	4	1	12.011	14.007	190.23	0.39	0.040
Os	26	4	1	12.011	14.007	190.23	0.34	0.032
Os	36	4	1	12.011	14.007	190.23	0.28	0.024
Os	44	4	1	12.011	14.007	190.23	0.25	0.020
Os	66	4	1	12.011	14.007	190.23	0.18	0.014
Os	92	4	1	12.011	14.007	190.23	0.14	0.010
Ir	2	4	1	12.011	14.007	192.22	0.71	0.143
Ir	8	4	1	12.011	14.007	192.22	0.56	0.077
Ir	12	4	1	12.011	14.007	192.22	0.49	0.059
Ir	20	4	1	12.011	14.007	192.22	0.39	0.040
Ir	26	4	1	12.011	14.007	192.22	0.34	0.032
Ir	36	4	1	12.011	14.007	192.22	0.28	0.024
Ir	44	4	1	12.011	14.007	192.22	0.25	0.020
Ir	66	4	1	12.011	14.007	192.22	0.18	0.014
Ir	92	4	1	12.011	14.007	192.22	0.14	0.010
Pt	2	4	1	12.011	14.007	195.08	0.71	0.143

Pt	8	4	1	12.011	14.007	195.08	0.56	0.077
Pt	12	4	1	12.011	14.007	195.08	0.49	0.059
Pt	20	4	1	12.011	14.007	195.08	0.40	0.040
Pt	26	4	1	12.011	14.007	195.08	0.35	0.032
Pt	36	4	1	12.011	14.007	195.08	0.29	0.024
Pt	44	4	1	12.011	14.007	195.08	0.25	0.020
Pt	66	4	1	12.011	14.007	195.08	0.19	0.014
Pt	92	4	1	12.011	14.007	195.08	0.14	0.010
Au	2	4	1	12.011	14.007	196.97	0.71	0.143
Au	8	4	1	12.011	14.007	196.97	0.56	0.077
Au	12	4	1	12.011	14.007	196.97	0.50	0.059
Au	20	4	1	12.011	14.007	196.97	0.40	0.040
Au	26	4	1	12.011	14.007	196.97	0.35	0.032
Au	36	4	1	12.011	14.007	196.97	0.29	0.024
Au	44	4	1	12.011	14.007	196.97	0.25	0.020
Au	66	4	1	12.011	14.007	196.97	0.19	0.014
Au	92	4	1	12.011	14.007	196.97	0.15	0.010

Table S4. Comparison of converged magnetic moments and energies for the bare FeN₄ structure and its *H, *OH, *O, and *OOH structures under different initial magnetic moment settings (0, 2, 4, 5).

Structure	Magnetic moment (μB)				Energy (eV)		
	0	2	4	5	$\Delta 2-0$	$\Delta 4-0$	$\Delta 5-0$
*							
FeN ₄ -I	0.055	1.606	1.606	1.606	-0.33	-0.33	-0.33
FeN ₄ -II	-0.031	1.816	1.816	1.816	-0.50	-0.50	-0.50
FeN ₄ -III	-0.217	1.899	1.899	1.899	-0.61	-0.61	-0.61
FeN ₄ -IV	0.580	1.848	0.418	-1.765	-0.39	0.01	-0.23
FeN ₄ -V	-0.365	0.378	-1.850	0.323	0.00	-0.51	0.04
FeN ₄ -VI	0.706	0.939	1.836	1.669	0.00	4.34	1.92
FeN ₄ -VII	1.528	1.853	-0.038	-1.853	-0.38	0.13	-0.38
FeN ₄ -VIII	-0.513	0.131	1.854	-1.855	0.03	-0.52	-0.52
FeN ₄ -IX	1.847	1.860	1.903	1.846	0.25	0.28	0.00
*H							
FeN ₄ -I	-0.001	0.140	0.140	-0.140	-0.01	-0.01	-0.01
FeN ₄ -II	0.000	0.883	0.883	0.883	-0.14	-0.14	-0.14
FeN ₄ -III	-0.014	1.020	1.020	1.020	-0.21	-0.21	-0.21
FeN ₄ -IV	0.000	0.781	0.781	0.781	-0.07	-0.07	-0.07
FeN ₄ -V	0.002	0.942	0.942	0.941	-0.17	-0.17	-0.17
FeN ₄ -VI	0.972	1.051	0.499	0.720	0.17	2.31	1.63
FeN ₄ -VII	0.015	0.913	-0.951	0.002	-0.13	-0.13	0.00
FeN ₄ -VIII	-0.954	-0.952	0.954	1.028	0.00	0.00	0.08
FeN ₄ -IX	0.940	0.001	0.048	-0.941	0.19	0.19	0.00
*OH							
FeN ₄ -I	0.027	2.262	2.262	2.263	-0.49	-0.49	-0.49
FeN ₄ -II	0.008	0.993	0.993	0.993	-0.27	-0.27	-0.27
FeN ₄ -III	-0.098	1.066	1.066	1.066	-0.31	-0.31	-0.31

FeN ₄ -IV	-0.013	1.038	1.038	1.038	-0.30	-0.30	-0.30
FeN ₄ -V	-1.014	1.015	1.015	1.015	0.00	0.00	0.00
FeN ₄ -VI	-1.080	1.566	2.483	2.472	0.95	2.33	2.07
FeN ₄ -VII	-1.036	1.036	1.037	1.037	0.00	0.00	0.00
FeN ₄ -VIII	1.078	1.077	1.567	1.436	0.00	0.95	0.21
FeN ₄ -IX	0.133	1.040	1.433	1.620	-0.33	-0.11	0.51

***O**

FeN ₄ -I	0.141	1.315	1.317	1.317	-0.34	-0.34	-0.34
FeN ₄ -II	1.213	1.213	1.213	1.213	0.00	0.00	0.00
FeN ₄ -III	-1.214	1.214	1.214	1.214	0.00	0.00	0.00
FeN ₄ -IV	-0.135	1.224	-0.074	1.224	-0.34	-0.01	-0.34
FeN ₄ -V	1.224	1.224	2.062	1.224	0.00	0.80	0.00
FeN ₄ -VI	-0.323	1.337	3.598	3.561	0.17	5.38	5.94
FeN ₄ -VII	0.541	-0.026	1.225	1.225	-0.11	-0.43	-0.43
FeN ₄ -VIII	1.221	1.221	1.221	1.467	0.00	0.00	0.17
FeN ₄ -IX	-0.128	1.226	-0.127	-0.127	-0.34	0.00	0.00

***OOH**

FeN ₄ -I	-0.172	0.988	0.989	0.988	-0.29	-0.29	-0.29
FeN ₄ -II	0.003	0.942	0.942	0.942	-0.28	-0.28	-0.28
FeN ₄ -III	0.006	0.805	0.805	0.805	-0.23	-0.23	-0.23
FeN ₄ -IV	0.959	0.960	0.960	0.960	0.00	0.00	0.00
FeN ₄ -V	0.017	0.947	0.947	0.947	-0.30	-0.30	-0.30
FeN ₄ -VI	-0.957	1.849	2.878	2.470	0.62	3.78	3.20
FeN ₄ -VII	-0.959	0.959	0.959	0.959	0.00	0.00	0.00
FeN ₄ -VIII	0.965	0.965	1.437	1.515	0.00	0.63	0.99
FeN ₄ -IX	0.031	0.963	1.236	1.344	-0.32	-0.17	-0.08

Table S5. Comparison of magnetic moments and energies for 3d metal-based MN₄-X single-atom catalysts under antiferromagnetic and ferromagnetic configurations.

Structure	Magnetic moment (μB)				Energy (eV)
	AFM(M1)	AFM(M2)	FM(M1)	FM(M2)	$\Delta(\text{FM-AFM})$
CoN ₄ -I	-0.498	0.498	0.507	0.507	0.020
CoN ₄ -II	-0.705	0.705	0.693	0.693	-0.028
CoN ₄ -III	-0.772	0.772	0.817	0.817	0.006
CoN ₄ -IV	-0.631	0.616	0.657	0.658	-0.010
CoN ₄ -V	-0.750	0.750	0.750	0.750	0.000
CoN ₄ -VI	-0.769	0.765	0.772	0.772	-0.160
CoN ₄ -VII	-0.848	0.848	0.849	0.849	0.002
CoN ₄ -VIII	-0.795	0.793	0.793	0.793	-0.001
CoN ₄ -IX	-0.769	0.769	0.574	0.574	0.070
CrN ₄ -I	-3.143	3.143	3.136	3.136	-0.090
CrN ₄ -II	-3.155	3.155	3.182	3.182	0.023
CrN ₄ -III	-3.215	3.215	3.230	3.230	0.040
CrN ₄ -IV	-3.223	3.223	3.217	3.217	-0.004
CrN ₄ -V	-3.224	3.224	3.230	3.230	0.010
CrN ₄ -VI	-3.218	3.218	3.223	3.223	0.013
CrN ₄ -VII	-3.235	3.235	3.238	3.238	0.006
CrN ₄ -VIII	-3.222	3.222	3.219	3.219	-0.008
CrN ₄ -IX	-3.232	3.232	3.233	3.233	0.003
CuN ₄ -I	0.000	0.000	0.193	0.193	-0.057
CuN ₄ -II	-0.497	0.497	0.521	0.521	0.020
CuN ₄ -III	-0.429	0.429	0.461	0.461	-0.038
CuN ₄ -IV	-0.523	0.523	0.525	0.525	0.007
CuN ₄ -V	-0.526	0.526	0.526	0.526	0.010
CuN ₄ -VI	-0.529	0.529	0.529	0.529	0.001
CuN ₄ -VII	-0.530	0.530	0.531	0.531	0.001
CuN ₄ -VIII	-0.532	0.532	0.533	0.533	0.000

CuN ₄ -IX	-0.534	0.534	0.533	0.533	0.000
FeN ₄ -I	-1.536	1.536	1.571	1.571	0.016
FeN ₄ -II	-1.820	1.820	1.804	1.804	0.001
FeN ₄ -III	-1.866	1.866	1.880	1.880	-0.040
FeN ₄ -IV	-1.705	1.705	1.843	1.843	-0.429
FeN ₄ -V	-1.848	1.848	1.848	1.848	0.001
FeN ₄ -VI	-1.859	1.859	1.860	1.859	0.010
FeN ₄ -VII	-1.854	1.854	1.854	1.854	0.000
FeN ₄ -VIII	-1.865	1.865	1.842	1.865	-0.010
FeN ₄ -IX	-1.848	1.848	1.849	1.848	0.016
MnN ₄ -I	-2.773	2.773	2.576	2.576	-0.027
MnN ₄ -II	-2.906	2.906	2.905	2.905	0.014
MnN ₄ -III	-2.966	2.965	2.963	2.963	-0.085
MnN ₄ -IV	-2.926	2.926	2.935	2.935	0.005
MnN ₄ -V	-2.923	2.923	2.918	2.918	-0.008
MnN ₄ -VI	-2.967	2.967	2.945	2.945	-0.018
MnN ₄ -VII	-2.920	2.920	2.919	2.919	-0.001
MnN ₄ -VIII	-2.942	2.942	2.934	2.934	-0.014
MnN ₄ -IX	-2.924	2.924	2.919	2.919	0.002

References

1. B. Hinnemann, J. K. Nørskov and H. Topsøe, *Phys. Chem. B*, 2005, **109**, 2245-2253.
2. Y. Wang, W. Qiu, E. Song, F. Gu, Z. Zheng, X. Zhao, Y. Zhao, J. Liu and W. Zhang, *Natl. Sci. Rev.*, 2017, **5**, 327-341.
3. S. Steinberg and R. Dronskowski, *Journal*, 2018, **8**.